Extending plasma channel of filamentation with a multi-focal-length beam

Zuofei Hong,[1] **Qingbin Zhang,**[1*] **S. Ali Rezvani,**[1] **Pengfei Lan,**[1] **and Peixiang Lu**[1,2,3]

[1]*Wuhan National Laboratory for Optoelectronics and School of Physics, Huazhong University of Science and Technology, Wuhan 430074, China*
[2]*Laboratory of Optical Information Technology, Wuhan Institute of Technology, Wuhan 430073, China*
[3]*lupeixiang@mail.hust.edu.cn*
[*]*zhangqingbin@mail.hust.edu.cn*

Abstract: We propose a novel scheme that lengthens the plasma channel in filamentation with a multi-focal-length beam. Instead of one focal length introduced by a conventional convex lens, the multi-focal-length beam modulated by a spatial light modulator (SLM) produces a filament in an extended range with limited but strictly manipulated laser energy. The results show that the scheme is capable of doubling the filament length compared to a single-lens scheme with a 2-mJ input pulse. The filament location and length can be simply tuned by altering the spatial amplitude and phase or employing higher energies. Furthermore, the extended filament length leads to the generation of a broadened continuum ranging from visible (VIS) to infrared (IR) domain. This versatile scheme offers an efficient tool for the development of a variety of applications involving ultrafast nonlinear optics.

OCIS codes: (320.2250) Femtosecond phenomena; (320.7110) Ultrafast nonlinear optics; (320.6629) Supercontinuum generation.

References and links

1. A. Braun, G. Korn, X. Liu, D. Du, J. Squier, and G. Mourou, "Self-channeling of high-peak-power femtosecond laser pulses in air," Opt. Lett. **20**, 73–75 (1995).
2. F. Krausz and M. Ivanov, "Attosecond physics," Rev. Mod. Phys. **81**, 163–234 (2009).
3. E. Goulielmakis, M. Schultze, M. Hofstetter, V. S. Yakovlev, J. Gagnon, M. Uiberacker, A. L. Aquila, E. M. Gullikson, D. T. Attwood, R. Kienberger, F. Krausz, and U. Kleineberg, "Single-Cycle Nonlinear Optics," Science **320**, 1614–1617 (2008).
4. L. He, P. Lan, Q. Zhang, C. Zhai, F. Wang, W. Shi, and P. Lu, "Spectrally resolved spatiotemporal features of quantum paths in high-order harmonic generation," Phys. Rev. A **92**, 043403 (2015).
5. L. He, Y. Li, Q. Zhang, and P. Lu, "Ultra-broadband water window supercontinuum generation with high efficiency in a three-color laser field," Opt. Express **21**, 2683–2692 (2013).
6. X. Ma, Y. Zhou, and P. Lu, "Multiple recollisions in strong-field nonsequential double ionization," Phys. Rev. A **93,** 013425 (2016).
7. M. Li, P. Zhang, S. Luo, Y. Zhou, Q. Zhang, P. Lan, and P. Lu, "Selective enhancement of resonant multiphoton ionization with strong laser fields," Phys. Rev. A **92**, 063404 (2015).
8. J. Kasparian, M. Rodriguez, G. Méjean, J. Yu, E. Salmon, H. Wille, R. Bourayou, S. Frey, Y.-B. André, A. Mysyrowicz, R. Sauerbrey, J.-P. Wolf, and L. Wöste, "White-light filaments for atmospheric analysis," Science **301**, 61–64 (2003).
9. Q. Luo, H. L. Xu, S. A. Hosseini, J. F. Daigle, F. Théberge, M. Sharifi, and S. L. Chin, "Remote sensing of pollutants using femtosecond laser pulse fluorescence spectroscopy," Appl. Phys. B **82**, 105–109 (2006).

#253983 Received 16 Nov 2015; revised 8 Feb 2016; accepted 17 Feb 2016; published 19 Feb 2016

10. H. L. Xu, and S. L. Chin, "Femtosecond laser filamentation for atmospheric sensing," Sensors **11**, 32–53 (2011).
11. P. Klarskov, A. C Strikwerda, K. Iwaszczuk, and P. U. Jepsen, "Experimental three-dimensional beam profiling and modeling of a terahertz beam generated from a two-color air plasma," New J. Phys. **15**, 075012 (2013).
12. J. Zhao, W. Chu, L. Guo, Z. Wang, J. Yang, W. Liu, Y. Cheng, Z. Xu, "Terahertz imaging with sub-wavelength resolution by femtosecond laser filament in air," Sci. Rep. **4,** 3880 (2014).
13. N. V. Vvedenskii, A. I. Korytin, V. A. Kostin, A. A. Murzanev, A. A. Silaev, and A. N. Stepanov, "Two-color laser-plasma generation of terahertz radiation using a frequency-tunable half harmonic of a femtosecond pulse," Phys. Rev. Lett. **112**, 055004 (2014).
14. L. Bergé, S. Skupin, C. Köhler, I. Babushkin, and J. Herrmann, "3D numerical simulations of THz generation by two-color laser filaments," Phys. Rev. A **110**, 073901 (2013).
15. S. L. Chin, and K. Miyazaki, "A comment on lightning control using a femtosecond laser," Jpn. J. Appl. Phys. **38** (2011).
16. R. Ackermann, G. Méchain, G. Méjean, R. Bourayou, M. Rodriguez, K. Stelmaszczyk, J. Kasparian, J. Yu, E. Salmon, S. Tzortzakis, Y. B. André, J. F. Bourrillon, L. Tamin, J. P. Cascelli, C. Campo, C. Davoise, A. Mysyrowicz, R. Sauerbrey, L. Wöste, and J. P. Wolf, "Influence of negative leader propagation on the triggering and guiding of high voltage discharges by laser filaments," Appl. Phys. B **82**, 561–566 (2006).
17. S. L. Chin, S. A. Hosseini, W. Liu, Q. Luo, F. Théberge, N. Aközbek, A. Becker, V. P. Kandidov, O.G. Kosareva, and H. Schroeder, "The propagation of powerful femtosecond laser pulses in optical media: physics, applications, and new challenges," Can. J. Phys. **83**, 863–905 (2006).
18. A. Couairon, and A. Mysyrowicz, "Femtosecond filamentation in transparent media," Phys. Rep. **441**, 47–189 (2007).
19. F. Théberge, W. Liu, P. Tr. Simard, A. Becker, and S. L. Chin, "Plasma density inside a femtosecond laser filament in air: strong dependence on external focusing," Phys. Rev. E **74**, 036406 (2006).
20. K. Lim, M. Durand, M. Baudelet, and M. Richardson, "Transition from linear- to nonlinear-focusing regime in filamentation," Sci. Rep. **4**, 7217 (2014).
21. S. Akturk, B. Zhou, M. Franco, A. Couairon, and A. Mysyrowicz, "Generation of long plasma channels in air by focusing ultrashort laser pulses with an axicon," Opt. Commun. **282**, 129–134 (2009).
22. X. Sun, T. Zeng, H. Gao, S. Zhang, and W. Liu, "Power dependent filamentation of a femtosecond laser pulse in air by focusing with an axicon," J. Phys. B: At. Mol. Opt. Phys. **48**, 094004 (2015).
23. Z. Song, Z. Zhang, and T. Nakajima, "Transverse-mode dependence of femtosecond filamentation," Opt. Express **17,** 12217–12229 (2009).
24. Z. Song, and T. Nakajima, "Formation of filament and plasma channel by the Bessel incident beam in Ar gas: role of the outer part of the beam," Opt. Express **18,** 12923–12938 (2010).
25. N. Kaya, M. Sayrac, G. Kaya, J. Strohaber, A. A. Kolomenskii, and H. A. Schuessler, "Filament propagation length of femtosecond pulses with different transverse modes," arXiv preprint arXiv: 1406.5570 (2014).
26. M.Scheller, M. S. Mills, M.-A. Miri, W. Cheng, J. V. Moloney, M Kolesik, P. Polynkin, and D. N. Christodoulides, "Externally refuelled optical filaments," Nat. Photon. **8**, 297–301 (2014).
27. M. Mills, M. Heinrich, M. Kolesik, and D. Christodoulides, "Extending optical filaments using auxiliary dress beams," J. Phys. B: At. Mol. Opt. Phys. **48**, 094014 (2015).
28. D. Abdollahpour, P. Panagiotopoulos, M. Turconi, O. Jedrkiewicz, D. Faccio, P. Di Trapani, A. Couairon, D. G. Papazoglou, and S. Tzortzakis, "Long spatio-temporally stationary filaments in air using short pulse UV laser Bessel beams," Opt. Express **17**, 5052–5057 (2009).
29. Z. F. Feng, W. Li, C. X. Yu, X. Liu, J. Liu, and L. B. Fu, "Extended laser filamentation in air generated by femtosecond annular Gaussian beams," Phys. Rev. A **91**, 033839 (2015).
30. L. Bergé, "Boosted propagation of femtosecond filaments in air by double-pulse combination," Phys. Rev. E **69,** 065601(R) (2004).
31. S. Tzortzakis, G. Méchain, G. Patalano, M. Franco, B. Prade, and A. Mysyrowicz, "Concatenation of plasma filaments created in air by femtosecond infrared laser pulses," Appl. Phys. B **76**, 609–612 (2003).
32. N. Kaya, J. Strohaber, A. A. Kolomenskii, G. Kaya, H. Schroeder, and H. A. Schuessler, "White-light generation using spatially-structured beams of femtosecond radiation," Opt. Express **20**, 13337–13346 (2012).
33. D. Walter, S. Eyring, J. Lohbreier, R. Spitzenpfeil, and C. Spielmann, "Spatial optimization of filaments," Appl. Phys. B **88**, 175–178 (2009).
34. F. Hagemann, O. Gause, L. Wöste, and T. Siebert, "Supercontinuum pulse shaping in the few-cycle regime," Opt. Express **21**, 5536–5549 (2013).
35. J. P. Vizcaíno, O. M.-Yero, R. B.-Varillas, G. M.-Vega, J. R. Vázquez de Aldana, and J. Láncis, "On-axis non-linear effects with programmable Dammann lenses under femtosecond illumination," Opt. Lett. **38**, 1621–1623 (2013).
36. W. Liu, F. Théberge, J.-F. Daigle, P.T. Simard, S.M. Sarifi, Y. Kamali, H.L. Xu, and S.L. Chin, "An efficient control of ultrashort laser filament location in air for the purpose of remote sensing," App. Phys. B **85**, 55–58 (2006).
37. L. Zhu, and J. Wang, Arbitrary manipulation of spatial amplitude and phase using phase-only spatial light modulators, Sci. Rep. **4,** 7441 (2014).

#253983 Received 16 Nov 2015; revised 8 Feb 2016; accepted 17 Feb 2016; published 19 Feb 2016

38. A. Couairon, E. Brambilla, T. Corti, D. Majus, O. de J. Ramírez-Góngora, and M. Kolesik, "Practitioners guide to laser pulse propagation models and simulation," Eur. Phys. J. Special Topics **199**, 5–76 (2011).
39. J. H. Marburger, "Self-focusing: Theory," Prog. Quant. Electr. **4**, 35–110 (1975).
40. L. Bergé, S. Skupin, and G. Steinmeyer, "Temporal self-restoration of compressed optical filaments," Phys. Rev. Lett. **101**, 213901 (2008).
41. L. Bergé, and S. Skupin, "Few-cycle light bullets created by femtosecond filaments," Phys. Rev. Lett. **100,** 113902 (2008).
42. G. Cerullo and S. De Silvestri, "Ultrafast optical parametric amplifiers," Rev. Sci. Instrum. **74,** 1–18 (2003).
43. M. Bradler, P. Baum, E. Riedle, "Femtosecond continuum generation in bulk laser host materials with sub-μJ pump pulses," Appl. Phys. B **97**, 561–574 (2009).
44. Z. Hong, Q. Zhang, P. Lan, and P. Lu, "Generation of few-cycle infrared pulses from a degenerate dual-pump OPCPA," Opt. Express **22**, 5544-5557 (2014).
45. F. Silva, D. R. Austin, A. Thai, M. Baudisch, M. Hemmer, D. Faccio, A. Couairon, and J. Biegert, "Multi-octave supercontinuum generation from mid-infrared fiamentation in a bulk crystal," Nature Commun. **3**, 807 (2012).
46. V. Jukna, J. Galinis, G. Tamosauskas, D. Majus, and A. Dubietis, "Infrared extension of femtosecond supercontinuum generated by filamentation in solid-state media," Appl. Phys. B **116,** 477–483 (2014).
47. P. Vasa, M. Singh, R. Bernard, A. K. Dharmadhikari, J. A. Dharmadhikari, and D. Mathur, "Supercontinuum generation in water doped with gold nanoparticles," Appl. Phys. Lett. **103**, 111109 (2013).
48. J. Darginavičius, D. Majus, V. Jukna, Nail Garejev, G. Valiulis, A. Couairon, and A. Dubietis, "Ultrabroadband supercontinuum and third-harmonic generation in bulk solids with two optical-cycle carrier-envelope phase-stable pulses at 2 μm," Opt. Express **21**, 25210–25220 (2013).
49. D. Kiselev, L. Woeste, and J.-P. Wolf, "Filament-induced laser machining (FILM)," Appl. Phys. B **100**, 515–520 (2010).
50. A. Valenzuela, C. Munson, A. Porwitzky, M. Weidman, and M. Richardson, "Comparison between geometrically focused pulses versus filaments in femtosecond laser ablation of steel and titanium alloys," Appl. Phys. B **116**, 485–491 (2014).
51. S. Butkus, D. Paipulas, D. Kaškelytė, E. Gaižauskas, and V. Sirutkaitis, "Improvement of cut quality in rapid-cutting of glass method via femtosecond laser filamentation," Journal of Laser Micro/Nanoengineering **10**, 59–63 (2015).

1. Introduction

Since the phenomenon of filamentation was first observed and reported by Braun et al. [1], it has attracted numerous attentions in various applications including high-order harmonic generation [2–5], ionization [6, 7], remote sensing [8–10], THz generation [11–14], and lightning control [15, 16], etc. A filament is generated when a laser beam with sufficient power propagates in a nonlinear medium [17, 18]. Due to the dynamic balance between Kerr self-focusing and plasma defocusing, the filament can persist several times longer than the diffraction length, leaving a row of plasma with the density of around 10^{16} /cm^3 and a lifetime of several nanoseconds. Generally, a collimated beam is capable of generating the longest plasma channel due to the absence of diffraction effect, which will also result in a very low plasma density. To increase the density of the plasma channel, the beam can be focused by a single convex lens. Previous researches have proved that an incident beam with a larger numerical aperture (NA) corresponds to a higher plasma density while sacrificing the filament length [19, 20].

Even though lengthy filaments have already been generated with collimated or lens-focused beams, the potential applications of filaments require further extending the plasma channel length while maintaining high plasma density. Various approaches other than using a single lens have been reported to achieve this goal. Compared to a Gaussian beam, a Bessel beam features a preferable non-diffractive propagation, leading to a high on-axis intensity over a longer distance. A quasi-Bessel beam can be produced by focusing a collimated Gaussian beam with an axicon. As previously studied in [21, 22], the axicon-focused quasi-Bessel beam can generate a relatively longer plasma channel compared to focusing with conventional lenses. The idea of filamentation with quasi-Bessel beam has been expanded to other non-Gaussian spatial modes. In [23–25], the authors employed beams with different transverse modes, e.g. Bessel-Gaussian beam (BGB), Laguerre-Gaussian beam (LGB), truncated Bessel beam (without the

#253983 Received 16 Nov 2015; revised 8 Feb 2016; accepted 17 Feb 2016; published 19 Feb 2016

side lobes), and the combination of two Gaussian modes. The results show that the filament induced by BGB and LGB is longer than the Gaussian beam under the same peak intensity, pulse duration and the radius of the central beam. The lengthening effect is found to be resulted from the outer part (side lobes) of the BGB and LGB that acts as the energy reservoir for the central beam. The filaments tend to be longer when there are more side lobes with more energy contained.

A new scheme that takes advantage of the energy reservoir was recently proposed and investigated in [26, 27]. The authors dressed a Gaussian beam with an auxiliary annular beam. The low-intensity Bessel "dressing" beam propagates linearly and constantly refuels the optical filament in the center. Consequently, the filament is prolonged to an order of magnitude longer than the undressed Gaussian case. It is found that the beam width and inward radial chirp play important roles in extending the filament whereas the spatial distribution of power in the dressing beam is only a minor influence. This approach is highly scalable by changing the initial parameters of the optical components, thus it can be applied in applications that require even further elongated filaments.

Another method for generating lengthy filament is to alter the effective focal length of the input beam [28]. The combination of a concave lens and an axicon can increase the range of the effective focus position for different radius components compared to a single convex lens or axicon. By using an annular Gaussian beam (or any beam with zero center intensity) as the input, this scheme can produce a filament that persists a distance of around 3 m [29]. The length of the plasma channel produced by a ring-Gaussian beam, compared to a Gaussian beam under the same initial condition, has a significant improvement.

Apart from extending the filament length from purely spatial point of view, efforts have also been made by optimizing the pulses temporally. As presented in [30, 31], the combination of two femtosecond converging pulses is capable of "boosting" the filamentation range. The two pulses are temporally delayed in order to achieve the concatenation of filaments created by each pulses. Their temporal delay is determined to guarantee that the second pulse starts self focusing when the ionization of the first pulse ends. In this way, the total length of the plasma channel could be nearly doubled accompanied with a broadband white-light emission.

It is noteworthy that the filament length is directly related to the input pulse energy and can be scaled up by raising the initial power. In [22], the authors found out that the length of filament increases almost linearly with the laser power. Using an axicon of 176° top angle, a filament length of nearly 30 cm is achieved with 3.5-mJ pulse energy. Further increasing energy of the input Gaussian pulse might produce multiple filaments at the high intensity area. By distributing the input energy to a central Gaussian beam (0.87 mJ) and a dressing quasi-Bessel beam (3.5 mJ), the filament is elongated to $\sim$2 m in [26]. If the whole 28 mJ energy were used in the dressing-beam scheme, the filament length can reach as long as 45 m according to the numerical simulation. Even though the filament generated from a dressed beam is intriguing when pulses with tens of millijoule energy are available, the possibility of extending filament length with relatively lower pulse energy (< 3 mJ) is still quite limited.

In this paper, we report a novel scheme that optimizes filamentation with a multi-focal-length beam. The initially collimated beam is modulated in a radius-dependent way by a spatial light modulator (SLM) [32–35] and the amplitude and phase are determined in order to combine components of different effective focal lengths. Due to the damage threshold of the liquid crystals in SLM, it is a suitable choice of modulating the beam for relatively low-energy filamentation. In a conventional single-lens scheme, the diffraction of the beam after focal point causes power loss at the edge of the main beam, which terminates filamentation. Whereas in the multi-focal-length scheme, the input beam contains a column of focal points and the energy flow is strictly manipulated by the initial spatial phase, which gives the beam a favorable

#253983 Received 16 Nov 2015; revised 8 Feb 2016; accepted 17 Feb 2016; published 19 Feb 2016

inherent self-balancing characteristic in the filament range, therefore the filamentation region is extended. In this case, the input energy will be more efficiently "locked" inside the filament and less energy is required for the generation of a longer plasma channel. Furthermore, since the spatial properties of the beam can be determined in any desired way, it is able to change the position of filamentation by simply programming the SLM. For the abovementioned works, the filament can only be generated in a different position when new optical components with different parameters are used, which adds complexity to the system. Comparatively, SLM offers an easier method for tuning of the location in filamentation. Moreover, the extended filament implies further accumulation of nonlinear effects, which will result in a favorable temporal-spectral characteristics. The rest of this paper is organized as follows. We illustrate the concept and numerical model in details in Sec. 2 and 3, respectively. Then in Sec. 4, we present the results and discuss the prospects. Finally, a conclusion is made in Sec. 5.

2. Concept

The basic idea of the proposed scheme is illustrated in Fig. 1. As depicted in the figure, a conventional convex lens focuses the incident light beam and produces a filament near the focal point, due to the sufficiently high intensity for the Kerr self-focusing effect. By changing the focal length of the lens, the filamentation will start at another distance with a different length. Mathematically speaking, the focusing effect of a lens is originated from the spatial phase introduced to the collimated beam. According to previous researches, the filamentation performance is determined by the beam propagation property, which can be improved by manipulating the spatial amplitude or phase of the incident beam in various approaches, e.g. filamentation with different transverse modes [23–25], auxiliary dressing beam [26, 27], annular beams [29], or telescope optics [36]. It is intuitively inferred that, if the spatial phases of different focal lengths are combined into one initial beam, a long filament that connects the relatively short filaments can be potentially realized.

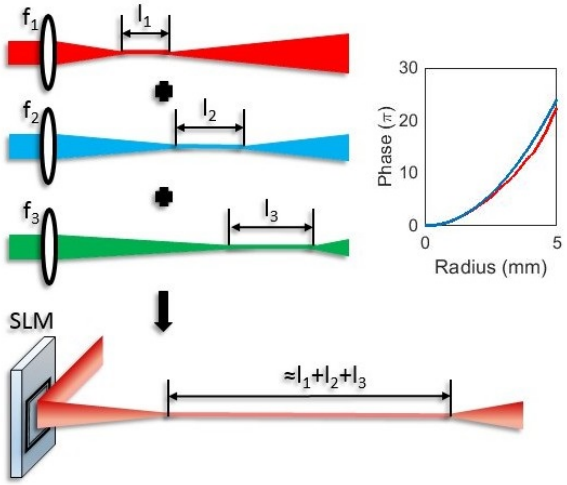

Fig. 1. Concept of the scheme.

Based on above illustrations, we propose a scheme that manipulates an initially collimated beam with SLM. Both the beam profile and phase are cylindrically symmetric in this scheme, therefore the spatial amplitude and phase are considered radius-dependent. For a single-focal-length beam, the focusing effect is attributed to the lens-induced spatial phase, which is written

#253983 Received 16 Nov 2015; revised 8 Feb 2016; accepted 17 Feb 2016; published 19 Feb 2016

as

$$\exp[i\phi(r)] = \exp(ik_0 r^2/2f), \tag{1}$$

with k_0 being the wave vector and f being the focal length. By combining several beams with varying energies and focal lengths, the spatial distribution of the superposed beam should be expressed as the summation of each of the single-focal-length beams, which is

$$A_{SLM}(r)\exp[i\phi_{SLM}(r)] = \sum_n A_n \exp(ik_0 r^2/2f_n), \tag{2}$$

where f_n is the effective focal lengths and A_n stands for different amplitudes of each components. The spatial amplitude and phase of the multi-focal-length beam can be therefore easily obtained as

$$\begin{aligned} A_{SLM}(r) &= |\sum_n A_n \exp(ik_0 r^2/2f_n)|, \\ \exp[i\phi_{SLM}(r)] &= \sum_n A_n \exp(ik_0 r^2/2f_n)/A_{SLM}(r). \end{aligned} \tag{3}$$

It can be seen from the above equations that the amplitude of a multi-focal-length beam $A_{SLM}(r)$, unlike a stable amplitude of the initial collimated beam, is radius-dependent. It is therefore deduced that not only phase modulation but also amplitude modulation will be required to produce a multi-focal-length beam.

In this article, we begin the investigations by selecting the effective focal length from 1.1 m to 1.5 m with an interval of 0.1 m, and the energies for each components are 100 μJ, 250 μJ, 400 μJ, 550 μJ, and 700 μJ, respectively. The reason for such energy arrangement will be explained later. With the given parameters, the spatial phase can be written as

$$\begin{aligned} A'(r) &= |\sum_{n=1}^{5} A_n \exp[ik_0 r^2/2(1+0.1n)]|, \\ \exp[i\phi'(r)] &= \sum_{n=1}^{5} A_n \exp[ik_0 r^2/2(1+0.1n)]/A'(r), \end{aligned} \tag{4}$$

in which $A_n = \sqrt{2I_n/c\varepsilon_0 n_0}$ represent the amplitudes of each components and $1+0.1n$ are the focal lengths. The radius-dependent phase is plotted as the red line in the inset of Fig. 1 in contrast with the blue line that shows the spatial phase introduced by a single lens ($f = 1.3$ m). Due to the coherent superposition of five components with different spatial phases, the combined spatial profile $A'(r)\exp(-r^2/\omega_r^2)$ (blue line in the cross section in Fig. 2(a)) is slightly different from the original Gaussian profile (black dashed line in the cross section in Fig. 2(a)). An energy loss around 20% is observed, implying that a collimated Gaussian beam with a pulse energy of 2.5 mJ would be necessary to produce the desired multi-focal-length beam. The pixel size of a commercially available SLM can be as small as 8 μm with a high resolution of 1920×1080, corresponding to an active area of 15.36×8.64 mm^2. A programmable SLM with such spatial resolution is capable of manipulating the beam in our desired way.

Fig. 2(a) and 2(b) show the calculated 2-dimensional (2D) spatial profile and phase of a multi-focal-length beam, respectively. The phase is the remainder of $\phi'(r)$ divided by 2π, hence an aperiodic ring shape is observed. An amplitude-and-phase SLM (e.g. Holoeye HEO 6001) is capable manipulating both the spatial profile and phase of a beam based on an image signal from a computer. As an alternative, by inputting the calculated amplitude and phase figures into the SLM, an initially collimated beam can be changed to a multi-focal-length beam. Furthermore, it has been reported that the amplitude and phase of a beam can be arbitrarily modulated by a combination of two phase-only SLMs [37], which shows that the desired modulation for a multi-focal-length is readily realizable with current technology.

#253983 Received 16 Nov 2015; revised 8 Feb 2016; accepted 17 Feb 2016; published 19 Feb 2016

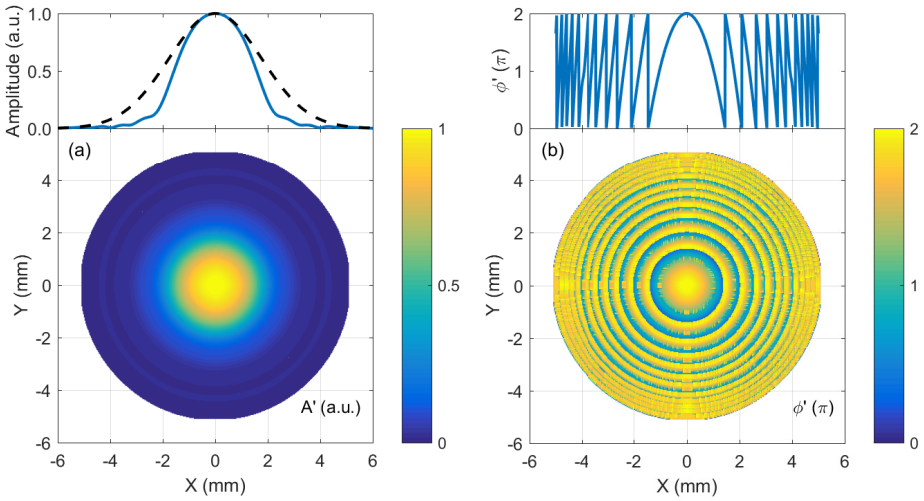

Fig. 2. Modulated amplitude (a) and phase (b) of a multi-focal-length beam.

3. Theory model

To quantitatively investigate the performance of this scheme, the filamentation process is simulated by numerically solving the nonlinear Schrödinger equation (NLSE) coupled with the plasma density evolution equation. We employ a linearly polarized laser electric field with cylindrical symmetry around the propagation axis. The incident beam with a Gaussian temporal profile and a modulated spatial profile can be expressed as:

$$\varepsilon(r,t,z=0) = A'(r)\exp(-r^2/\omega_r^2)\exp(-t^2/\tau_0^2)\exp[i\phi'(r)], \tag{5}$$

where ω_r and τ_0 are the half width at $1/e^2$ of the peak intensity spatially and temporally, respectively.

The nonlinear Schrödinger equation in the reference frame moving at the group velocity ($t = t_{lab} - zk'$), can be written as [38]:

$$\begin{aligned}\frac{\partial}{\partial z}\varepsilon =& \frac{i}{2k_0}T^{-1}\Delta_\perp\varepsilon + \sum_{l=2}^{4}\frac{ik^{(l)}}{l!}\frac{\partial^l}{\partial t^l}\varepsilon + \frac{ik_0n_2}{n_0}T[(1-f)|\varepsilon(t)|^2 + f\int_{-\infty}^{t}R(t-t')\left|\varepsilon(t')\right|^2dt']\varepsilon \\ &- \frac{ik_0}{2n_0^2\rho_c}T^{-1}\rho\varepsilon - \frac{\varepsilon}{2}(\sigma\rho + \sum_{m=O_2,N_2}\beta^{K_m}|\varepsilon|^{2K_m-2}).\end{aligned} \tag{6}$$

In the above equation, $\Delta_\perp$ is the Laplace operator, $k^{(l)}$ is the chromatic dispersion coefficient up to the 4th order, $n_2 = 1*10^{-23}\mathrm{m}^2/\mathrm{W}$ is the nonlinear refractive index, $\rho_c = \frac{\omega_0^2 m_e \varepsilon_0}{e^2} = 1.74*10^{27}/\mathrm{m}^3$ is the critical plasma density, the constant $\sigma = \frac{ke^2}{\omega m \varepsilon_0}\frac{\tau}{1+(\omega\tau)^2} = 5.47*10^{-24}\mathrm{m}^2$ corresponds to the cross-section for electron-neutral inverse bremsstrahlung ($\tau = 350$ fs being the electron-atom relaxation time) and $\beta^K = K\hbar\omega_0\rho_{at}\sigma_K$ is the coefficient of multiphoton absorption, $K = mod(\frac{U_i}{\hbar\omega_0}) + 1$ being the minimum of the photon number necessary to ionize the medium. The operator $T = 1 + i/\omega_0\frac{\partial}{\partial t}$ ensures that the model is valid even for few-cycle pulses, corresponding to a frequency domain representation of $\widehat{T} = 1 + \omega/\omega_0$. $R(\tau) = \tau_k^{-1}\exp(-\tau/\tau_k)$

#253983 Received 16 Nov 2015; revised 8 Feb 2016; accepted 17 Feb 2016; published 19 Feb 2016

with a characteristic time $\tau_k = 70$ fs stands for the Raman-delayed Kerr effect, the fraction of which is $f = 0.5$. The NLSE is coupled with the plasma evolution equation:

$$\frac{\partial}{\partial t}\rho_l = W(I)(\rho_{at,l} - \rho_l) + \frac{\sigma}{U_{i,l}}\rho_l I - \alpha\rho_l^2, l = O_2, N_2, \tag{7}$$

where $W(I)$ denotes the multiphoton ionization rate and $\alpha = 7 * 10^{-13}/(\mathrm{m}^3\mathrm{s})$ is the recombination rate, $\rho_{at,N_2} = 2 * 10^{25}/\mathrm{m}^3$ and $\rho_{at,O_2} = 5 * 10^{24}/\mathrm{m}^3$. The plasma defocusing effect is included in the NLSE as the summation of both gasses:

$$\rho = \rho_{O_2} + \rho_{N_2}. \tag{8}$$

The NLSE is computed with the split-step Fourier algorithm. We use the Crank-Nicholson method for calculating the linear effects, i.e. beam diffraction and dispersion, in the spectral domain, while the nonlinear effects are calculated in the time domain as:

$$\varepsilon(r,t,z+dz) = \varepsilon(r,t,z) \cdot \exp[N(\varepsilon)dz], \tag{9}$$

where $N(\varepsilon)$ stands for the summation of all the nonlinear terms. The step length dz is decided according to the peak intensity of the beam to ensure that $N(\varepsilon)dz \ll 1$ so that the algorithm is valid. In our simulation, the initial dz is selected to 2 mm and it is decreased to 20 μm during the filamentation. For the plasma, an Euler method is employed to integrate the plasma density evolution with respect to the time delay.

The simulation is performed in air using a laser beam centered at 800 nm with a FWHM temporal duration of 40 fs ($\tau_{FWHM} = \sqrt{2ln(2)}\tau_0$), the initial radius of the beam is ω_r = 3 mm. The pulse energy and effective focal length are variable and will be illustrated in detail in the following discussions.

4. Results and discussion

To start with, we assume a laser pulse with the energy of 2 mJ and effective focal length varying from 1.1 m to 1.5 m, the interval between each of them is 0.1 m, indicating that the initial beam contains five different focal-length components. The process is numerically simulated and the evolutions of the on-axis peak intensity, plasma density and fluence of the multi-focal-length filamentation are depicted in Fig. 3. To determine the lengthening effect of modulating the spatial amplitude and phase, the peak intensity and plasma density evolutions of single-lens schemes are plotted in Fig. 3(a) and 3(b) for comparison. All other parameters for the single-lens schemes are identical to the multi-focal-length scheme except the focal lengths, which are 1.1 m, 1.3 m, and 1.5 m,respectively. As observed in the figure, focusing the beam with a lens can produce a stable plasma channel (less than 10 % fluctuation) around the focal point with a length of 10$\sim$20 cm. On the contrary, the multi-focal-length beam generates a filament of over 50 cm, which is more than twice longer of the single-lens schemes. With the considered parameters, the peak intensity during filamentation approaches 4×10^{13} W/cm^2 and the plasma density exceeds 2×10^{16} /cm^3. The full width at 1/e^2 maximum of the beam fluence is kept around 200 μm with a fluctuation less than 20% in longer than 50-cm range.

Note that the modulated beam is equivalent to 5 beams with different focal lengths, sharing the total input energy. Based on Marburger's self-focusing theory [39], the power threshold for Kerr self-focusing is written as $P_{cr} \equiv 3.72\lambda^2/8\pi n_0 n_2$, corresponding to 7.89 GW in the studied case. A pulse energy of $\sim$300 μJ is required to trigger filamentation. It is observed in Fig. 3(a) and 3(b), even though the energy for $f = 1.1/1.2$ m components are insufficient for self-focusing, filamentation can take place with the assistance of the energy reservoir formed by longer focal-length components. In fact, the superposition of 5 focal-length components is

#253983 Received 16 Nov 2015; revised 8 Feb 2016; accepted 17 Feb 2016; published 19 Feb 2016

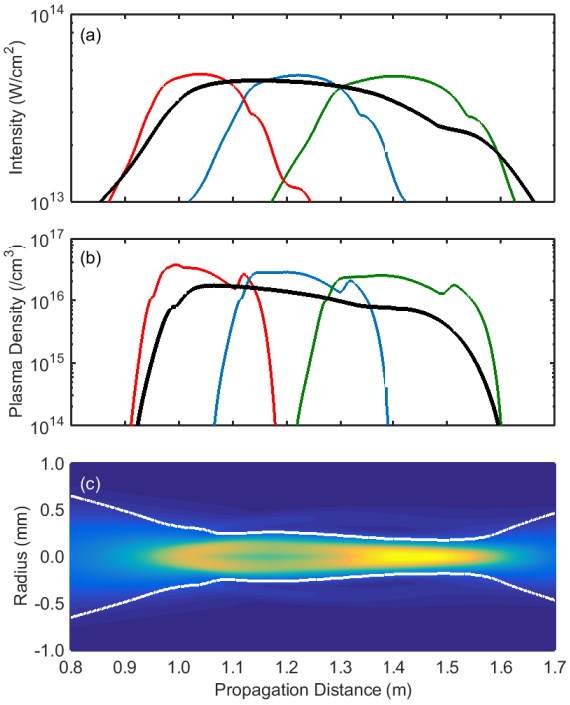

Fig. 3. (a) On-axis peak intensity, (b) plasma density, and (c) fluence evolutions of the multi-focal-length filamentation in comparison with the single lens scheme. The peak intensity and plasma density of single lens schemes are compared in (a) and (b), in which the focal lengths are 1.1 m, 1.3 m, and 1.5 m for the red, blue, and green lines, respectively. White lines in (c) indicate the beam radius during propagation.

so intense that the medium gets ionized even before the first effective focal length. As shown in Fig. 3(c) around $z = 1.2$ m region, the plasma defocusing becomes dominant due to the rapid increase of the intensity and the combined beam is slightly defocused from the center, which lasts until after $z = 1.3$ m. For this reason, more energy are arranged to longer focal-length components to ensure that the "refocusing" will occur after the defocusing around short focal lengths. After the beam is refocused, the long focal-length components start to take over while the previously diverged short focal-length components act as the energy reservoir. According to previous studies, the filamentation process is sustainable as long as the power within the main beam is above the critical power for self-focusing effect [27]. Owing to the energy reservoir formed by different components, every one of them will be able to generate a filament and will connect with each other. Consequently, a filament length that none of the single-lens scheme could produce alone is achieved.

Since the termination of the filament is resulted from the dissipation of the beam energy, it is reasonable to infer that the performance of the proposed scheme can be significantly improved by increasing the input pulse energy. The energy dependence of the proposed scheme is studied and plotted in Fig. 4(a). The input pulse energy are 2 mJ (blue line), 3 mJ (red line), 4 mJ (yellow line), and 5 mJ (purple line), respectively. With more sufficient input power, the filamentation begins even before approaching the first effective focal length. As a result, the filament length can be increased to nearly 1 m. Unlike the significant improvement before $z = 1$ m, the plasma

#253983 Received 16 Nov 2015; revised 8 Feb 2016; accepted 17 Feb 2016; published 19 Feb 2016

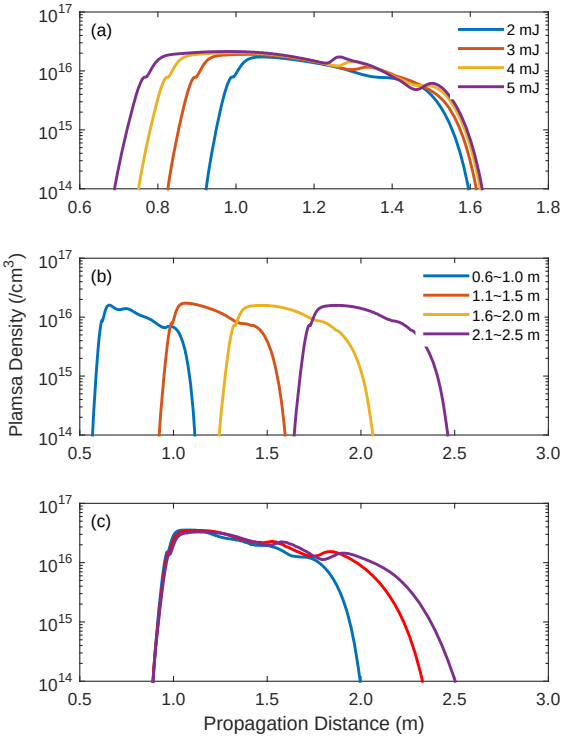

Fig. 4. Tunability of the multi-focal-length scheme by changing (a) input pulse energy and (b) effective focal lengths. (c). Blue line: energy 4 mJ, focal length 1.0∼1.8 m with 0.2-m interval, red line: energy 5 mJ, focal length 1.0∼2.2 m with 0.3-m interval, purple line: energy 5 mJ, focal length 1.0∼2.6 m with 0.4-m interval.

density evolution at the filament tail is barely different in four cases. Even though the pulse energy is increased, the longer focal-length components are still defocused by the intense plasma channel at the beginning of the filament. In order to more efficiently extend the filament at the tail, the energy distribution for different focal lengths has to be further optimized.

Tuning the filament location is of importance when applied in remote sensing [36]. Here we investigate the possibility of altering the filament location in the multi-focal-length scheme and the result is depicted in Fig. 4(b), the parameters are the same as in Fig. 3 except the effective focal lengths. Given a different spatial amplitude and phase, the filament can be generated at either shorter or further distances. When the focal lengths are changed to 0.6∼1.0 m, 1.6∼2.0 m, and 2.1∼2.5 m with the same interval of 0.1 m, the filaments are produced at corresponding positions. According to the relationship between filament length and initial numerical aperture (NA), longer effective focal lengths (smaller NA) is beneficial for a longer filament. The filament produced around $z = 2$m is able to reach a length of over 80 cm. This implies the possibility of simply tuning the filament position by programming the SLM differently. Compared to changing optical components, the programmable spatial phase offers much more convenience in tunability.

The results in Fig. 4(b) have shown the availability of generating filament with only 2-mJ pulse energy. For each of the focal-length components, higher energy corresponds to longer

#253983 Received 16 Nov 2015; revised 8 Feb 2016; accepted 17 Feb 2016; published 19 Feb 2016

filaments. Therefore, the interval between each effective focal length can be lengthened when the pulse energy is increased, resulting in an even longer plasma channel. In Fig. 4(c), the interval is increased to 0.2 m (blue line), 0.3 m (red line), and 0.4 m (purple line), respectively. To ensure that filaments produced from different focal-length components are connected, the input pulse energy are increased. Detailed parameters can be found in the caption of Fig. 4. In this way, the plasma channels are efficiently extended to over 1.5 m with no obvious gap between different effective focal lengths. Based on above results, it is proven that elongated filaments with simple tunability and energy scalability is readily available with the proposed multi-focal-length scheme.

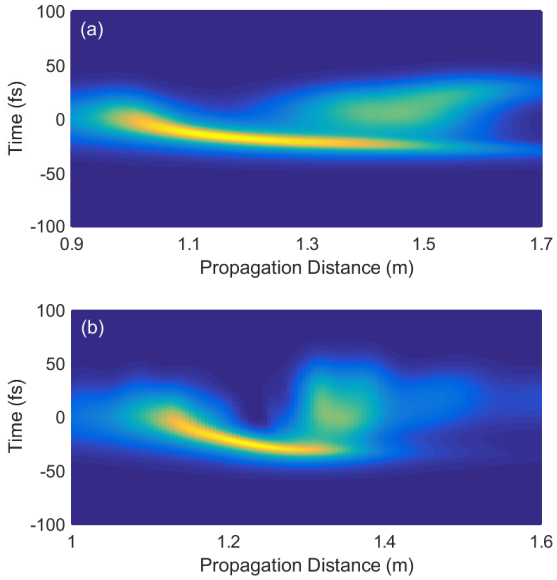

Fig. 5. The temporal distribution of the pulse with respect to the propagation distance in the multi-focal-length scheme (a) and single-lens scheme (b).

Throughout the development of filamentation, the temporal property of the laser pulse in filamentation has been studied in plenty of researches [40, 41]. Other than the filament length and plasma density, we have also investigated the pulse temporal evolution in the proposed scheme. Figure 5(a) shows the temporal profile with respect to the propagation distance in the multi-focal-length scheme, the parameters are identical to the ones used in Fig. 3. The pulse shape remains unchanged until around $z = 0.9$ m because the intensity is not high enough for Kerr self-focusing and the pulse propagation is only affected by diffraction and dispersion. After that, the intensity exceeds the critical point, thus self-compression and self-steepening occur. Due to the intensity dependent refractive index $\Delta n = n_2 I$, the less intense trailing edge of the pulse has a lower refractive index than the intensity peak when n_2 is positive, therefore it travels faster than the peak, leading to the steepening at the trailing side of the pulse. Meanwhile, the leading edge of the pulse ionizes the medium and generates plasma, which defocuses the trailing edge and results in a self-compressed pulse. The rapid compression of the pulse mainly takes place in the range between $z = 1.0$ m and $z = 1.2$ m, where all focal-length components are contributing to the focusing of the whole beam. The self-compressed pulse starts to stabilize after $z = 1.3$ m because the short focal-length components are already diverged, which slows

#253983 Received 16 Nov 2015; revised 8 Feb 2016; accepted 17 Feb 2016; published 19 Feb 2016

down the further focusing and compressing of the leading pulse. In the meantime, the previously defocused trailing side of pulse is refocused, leading to a second peak and a temporally-splitted pulse.

In comparison, the temporal evolution of a pulse focused by a $f = 1.3$ m lens is studied and depicted in Fig. 5(b). Phenomena including self-compression, pulse-splitting and self-steepening are observed. The leading side is self-compressed during filamentation and the trailing side refocuses into a splitted pulse, which are similar to Fig. 5(a). Nevertheless, the beam eventually diverges because of the diffraction after focal point and the peak intensity decreases, therefore the filament vanishes and the temporal evolution of the pulse stops. On the contrary, instead of being diverged, the filament in the multi-focal-length scheme is sustained by the subsequently focusing longer focal-length components and the refocused trailing pulse is continuously compressed. More detailed properties of the output pulses are analyzed in Fig. 6.

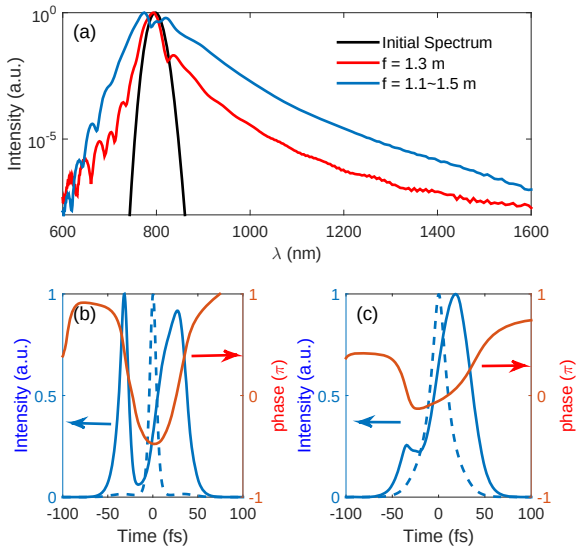

Fig. 6. (a). Black line is the initial spectrum, blue and red lines are the output spectra in multi-focal-length scheme and single-lens scheme, respectively. (b) and (c). Temporal shape (blue solid lines) and phase (red lines) of the output pulses in multi-focal-length scheme and single lens scheme, respectively. The FWHM duration of the transform limited pulses (blue dashed lines) are 8.2 fs and 20.1 fs, respectively.

The spectral characteristic of filamentation is favorable for its uses in atmospheric sensing [10] or optical parametric amplification (OPA) [42–44]. Owing to the continuous pulse compression during the filamentation, a broadband continuum can be expected correspondingly. The output spectrum of the multi-focal-length scheme is depicted in Fig. 6(a) (blue line) in comparison with the output spectrum of single-lens scheme (red line) and the initial spectrum (black line). As observed in the figure, spectra in both schemes are remarkably broadened and broadband continuums are obtained. Comparatively, the continuum produced in the proposed scheme is more than one order of magnitude higher than that in the single-lens schemes in both VIS and IR regions. It is known that the spectral broadening in filamentation mainly originates from the self-phase modulation (SPM) effect, which is directly related to the Kerr effect. Similar to the temporal evolution discussed above, the spectrum in single-lens scheme gets broadened when Kerr self-focusing and filamentation occurs. As the pulse passes the focal

#253983 Received 16 Nov 2015; revised 8 Feb 2016; accepted 17 Feb 2016; published 19 Feb 2016

point and the beam is diverged, the peak intensity decreases and broadening of the spectrum weakens. In the multi-focal-length scheme, even though the peak intensity is slightly lower than that in the single-lens scheme and the nonlinear effects are less intense, the filamentation lasts a much longer range for the SPM effect to accumulate. As a consequence, the spectrum is further broadened. The broadband continuum can significantly benefit applications such as remote sensing with Light Detection and Ranging (LIDAR) technique [8] and white-light seed generation in OPA systems [42].

The compressibility of output pulses from both schemes are discussed in Fig. 6(b) and 6(c). The uncompressed pulses from two schemes have similar durations. However, the temporal phase in Fig. 6(b) is close to a quadratic curve in the splitted pulses, which represents a much larger chirp than the almost linear temporal phase of the main pulse in Fig. 6(c). Therefore, after compensating the temporal chirp of each pulses, a transform limited pulse of 8.2 fs (three cycles) is obtained in the proposed scheme while the output pulse in the single-lens scheme can only be compressed to a duration of 20.1 fs.

Experiments of white-light continuum generation induced by laser filaments have been widely implemented not only in gas but also in solid or liquid mediums [32, 41, 45–48]. The condensed medium, compared to atmospheric gas, is a much denser material with orders of magnitude higher nonlinearity. Therefore, the supercontinuum can be generated with less pulse energy in a shorter distance and the bandwidth is much more efficiently broadened. As revealed by the above results, the multi-focal-length scheme is more beneficial for a broad output spectrum than the single-lens scheme in air. It implies the potential availability of applying the phase-modulated beam on a solid-state material for the generation of an ultra-broadband continuum. On the other hand, laser filament has been recognized as an useful tool in rapid-cutting [49–51]. The clamped high-intensity structure with a stable diameter offers a suitable method of precisely cutting metals or biological materials. The proposed scheme preserves all advantages of the conventional filamentation, meanwhile it allows the possibility of cutting thicker materials with higher tunability.

5. Conclusion

In conclusion, we have theoretically investigated the performance of a lengthened optical filament generated from a multi-focal-length beam. Various phase components of different focal lengths are contained in the initial spatial phase, leading to filamentation in an extended range. The length of the plasma channel is significantly prolonged compared to the conventional single-lens scheme with the same input energy, pulse duration, and beam diameter. During filamentation, the filament at a certain focal length can benefit from the energy reservoir formed by other components and get extended, therefore the filaments at different positions can be connected and combine a much longer filament. Owing to the strict manipulation of beam propagation by modulating the spatial amplitude and phase, the filament is efficiently generated with very limited laser power. Besides, the filament is easily tunable to a different distance in the proposed scheme by programming the SLM and increasing the input pulse energy. The potential of producing stable filaments in a wide range has been studied. In addition, a further broadened continuum is obtained as a result of the constant accumulation of nonlinear effects in the extended filament. The spectral-temporal performance implies a promising potential of supercontinuum generation in mediums with higher nonlinearity. The multi-focal-length scheme is also a potentially useful tool for laser-cutting of thick materials.

Acknowledgment

This work was supported by the NNSF of China under grants 11574101, 11204095, 11234004 and 61275126.

#253983 Received 16 Nov 2015; revised 8 Feb 2016; accepted 17 Feb 2016; published 19 Feb 2016